Photophysical and Electron Transfer Properties of $C_{60}(C_6H_5)_5OH$ and $C_{60}(C_6H_4F)_5OH$: A Laser Flash Photolysis and Pulse Radiolysis Study

Dipak K. Palit,*,† H. Mohan,† Paul R. Birkett,‡ and Jai P. Mittal†,§

Radiation Chemistry and Chemical Dynamics Division, Bhabha Atomic Research Centre, Trombay, Mumbai 400 085, India, and Fullerene Science Centre, The School of Chemistry, Physics and Environmental Science, University of Sussex, Brighton, BN1 9QJ, U.K.

Received: July 23, 1999; In Final Form: September 28, 1999

Photophysical properties of the excited singlet and triplet states of pentaphenylfulleren-2-ol ($C_{60}(C_6H_5)_5OH$, PPF) and penta-4-fluorophenylfulleren-2-ol [$C_{60}(C_6H_4F)_5OH$, PFPF], two derivatives of buckminsterfullerene, C_{60}, have been investigated in benzene and benzonitrile solutions using two complementary transient absorption techniques, namely, laser flash photolysis and pulse radiolysis. Singlet−singlet and triplet−triplet absorption spectra have been characterized. Quantum yields for formation of the triplet states by intersystem crossing from the singlet states, and also the intrinsic lifetimes of the singlet and triplet states, have been determined. In addition to the intrinsic decay of the triplet state, the evidences have been obtained for the contribution of the other two processes, namely, the self-quenching by the ground state and the T−T annihilation reaction, toward the decay of the triplet state, and the rate constants for these processes have been determined. The formation of charge transfer (CT) complexes with two aromatic amines, diphenylamine (DPA) and triphenylamine (TPA), in benzonitrile and the electron transfer reactions in the excited singlet and CT complexes have been studied.

Introduction

In recent years buckminsterfullerene, fullerene[60], and its derivatives have shown very promising applications in nonlinear optics (NLO) and optoelectronics,[1,2] photovoltaic cells,[3,4] and also in biology.[5−7] Fullerene[60] is considered to be an efficient photosensitizing agent in photodynamic therapy because of its ability to produce the triplet state with unit efficiency under photoexcitation.[8−15] Fullerenes also show various interesting properties, such as superconductivity,[16] ferromagnetism,[17] and photoconductivity[18] when they are chemically treated with some electron donors or acceptors. However, all of the applications mentioned here require a good knowledge of the photophysical and photochemical properties of their excited states, which are responsible for those important properties. For example, there have been extensive investigations of the optical limiting properties of the fullerenes in order to develop an understanding of the mechanism of optical limiting performance.[1,19,20] McLean et al.[19] used a five-level model, involving the S_0, S_1, S_n, T_1, and T_n states of the fullerene molecule for reverse saturable absorption in order to correlate the observed optical limiting responses with the ground ($S_0 \rightarrow S_1$) and excited state ($S_1 \rightarrow S_n$ and $T_1 \rightarrow T_n$) absorption cross sections of the fullerene. However, in a recent report Riggs and Sun[20] have suggested that significant optical limiting contributions are related to the bimolecular excited-state processes of the fullerenes, such as triplet−ground-state interaction and triplet−triplet annihilation reaction. This fact empasizes the need for thorough study of the photophysical properties of the fullerenes.

Investigations in recent years have confirmed that the nature of the functional groups and the degree of functionalization of the fullerene molecule severely affect its physicochemical properties,[21−26] and hence the fullerene chemistry has also been developed for introducing different organic functional groups into the molecule.[27−36] These functionalized fullerene molecules have enhanced properties, which improve the possibility of their application in the NLO field. The physicochemical properties of these fullerene derivatives have been shown to be very different from pristine fullerene[60] and this effect has been rationalized in terms of the perturbation of the electron distribution on the surface of the spherical molecule due to the presence of the functional groups.[37] The functionalization of the fullerenes has led to derivatives with increased solubility in water,[38−50] modified electron transfer,[56,57] and better nonlinear optical properties.[51−56] The increased solubility of the fullerenes in water provides the flexibility for their use in photodynamic therapy. However, due to the introduction of the functional groups onto the fullerene[60], two important properties, namely the quantum yield and the lifetime of the triplet state, which are responsible for high quantum yield of singlet oxygen in the photochemical reactions involving the fullerene[60], are reduced considerably.[57−59] Water-soluble fullerenes also show strong aggregation properties in aqueous solutions.[56] Pyrrolidino fullerenes have recently been shown to have excellent nonlinear properties[60] and efficient photocurrent response.[61] Even the photophysical and photochemical properties of the hydrogenated fullerenes, e.g., $C_{60}H_{18}$ and $C_{60}H_{36}$ have been shown to be significantly different from those of pristine fullerene.[58,59]

The Fullerene Science Centre at the University of Sussex, U.K. has synthesized a series of pentaaryl derivatives of fullerene[60] in which the nonlinear and electron transfer properties are expected to be significantly modified. Recently we have reported the results of our investigations of the photophysical and photochemical properties of one of these derivatives, namely monochloropentaphenylfullerene, $C_{60}(C_6H_5)_5Cl$ (MCPPF).[57] In this present paper the photophysical

* Corresponding author e-mail: dkpalit@apsara.barc.ernet.in. Fax: 91-22-5505150.

† Bhabha Atomic Research Centre, Mumbai.

‡ University of Sussex, U.K.

§ Also affiliated as the Honorary Professor with the Jawaharlal Nehru Centre for Advanced Scientific Research, Bangalore, India.

10.1021/jp992572f CCC: $18.00
Published on Web 11/20/1999

SCHEME 1

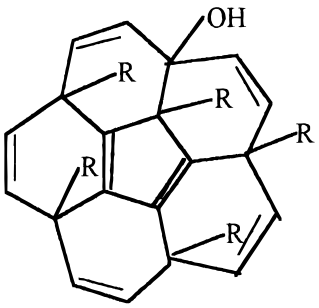

$R = C_6H_5$; $C_{60}(C_6H_5)_5OH$

$R = C_6H_4F$; $C_{60}(C_6H_4F)_5OH$

and photochemical properties of the other two derivatives of the same series, namely, pentaphenylfulleren-2-ol ($C_{60}(C_6H_5)_5OH$, PPF) and penta-4-fluorophenylfulleren-2-ol [$C_{60}(C_6H_4F)_5OH$, PFPF], are being reported. We also report the electron transfer reactions between these fullerene derivatives and two simple aromatic amines, namely, diphenylamine (DPA) and triphenylamine (TPA).

Experimental Section

Spectroscopic grade cyclohexane, benzene (BZ), and benzonitrile (BN) were obtained from Spectrochem, India and were used without further purification. All other chemicals used were of Analar grade purity. IOLAR grade N_2 (Indian Oxygen, 99.9% purity) was used to deaerate the samples prior to the pulsed experiments. Preparation and characterization of PPF and PFPF, the chemical structure of which has been presented in Scheme 1, will be reported elsewhere.[62] Steady-state optical absorption spectra were recorded on a Shimadzu model UV-160A spectrophotometer.

Laser Flash Photolysis. For picosecond laser flash photolysis experiments, the second (532 nm) or the third (355 nm) harmonic output pulses of 35 ps duration from an active−passive mode-locked Nd:YAG laser (Continuum, model 501-C-10) were used for excitation. Continuum probe pulses in the 400−920 nm region were generated by focusing the residual fundamental in an H_2O/D_2O mixture (50:50). The probe pulses were delayed with respect to the pump pulses using a 1 m long linear motion translation stage, and the transient absorption spectra at different delay times (up to 6 ns) were recorded by an optical multichannel analyzer (Spectroscopic Instruments, Germany) interfaced to an IBM PC. At the zero delay position, the probe light reaches the sample just after the end of the pump pulse. Transients surviving beyond 50 ns were studied by monitoring their absorption using a tungsten filament lamp in combination with a Bausch and Lomb monochromator (f/10, 350−800 nm), Hamamatsu R 928 PMT, and a 500 MHz digital oscilloscope (Tektronix, TDS-540A) connected to a PC.

For recording fluorescence spectra the samples were excited by 355 nm laser pulses (1 mJ) from the same picosecond laser, and the fluorescence emission was collected at the direction perpendicular to that of excitation through the optical fiber and the spectra were recorded by the optical multichannel analyzer. The spectra being reported here are not further corrected for the spectrograph transmission and the wavelength response function of the diode array detector.

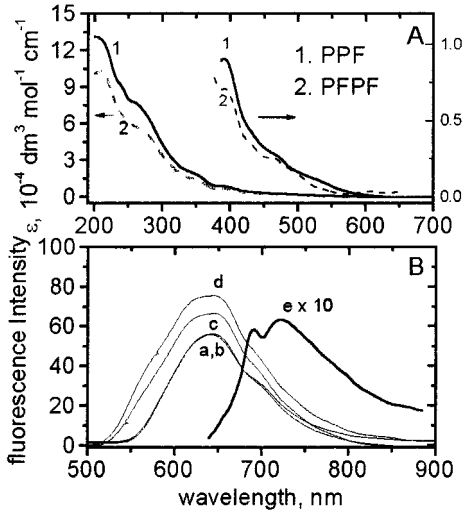

Figure 1. (A) Ground-state absorption spectra of PPF (1) and PFPF (2) in cyclohexane. (B) Fluorescence spectra of (a) PPF in BZ, (b) PFPF in BZ, (c) PFPF in BN, (d) PPF in BN, and (e) C_{60} in BZ.

Pulse Radiolysis. High energy (7 MeV) electron pulses of 50 ns duration, generated by a linear electron accelerator (Ray Technology, U.K.), were used for pulse radiolysis experiments. The transient species produced by the electron pulses were detected by monitoring the optical absorption. The absorbed dose from each pulse was determined using the aerated KSCN solution with $G\epsilon = 21520$ dm^3 mol^{-1} cm^{-1} for 100 eV of absorbed dose (the G value is the number of radicals or molecules produced per 100 eV of absorbed energy and ϵ is the molar absorptivity at 500 nm for the transient $(SCN)_2^{\bullet -}$.

Results and Discussion

A. Absorption and Fluorescence Characteristics. Both PPF and PFPF are soluble in benzene, toluene, benzonitrile, and alkane solvents, sparingly soluble in acetonitrile, but insoluble in water. The electronic absorption spectra of the two fullerene derivatives in cyclohexane are presented in Figure 1A. The absorption spectra of both of the molecules have similar features with the absorption peaks at 215, 231, and 255 nm and weak shoulders in the 330−370, 380−430, and 450−550 nm regions. These features are very similiar to those of $C_{60}(C_6H_5)_5Cl$ as reported earlier.[57] The absorption peaks of C_{60} in cyclohexane at 231, 257, and 329 nm are very sharp as compared to the absorption peaks of these three fullerene derivatives. Also, the absence of the broad and relatively strong absorption band in the 440−670 nm region in the absorption spectra of these fullerene derivatives suggests that the presence of the functional groups $(C_6H_5)_5OH$ and $(C_6H_4F)_5OH$ has considerably distorted the electronic structure of the parent molecule. Both PPF and PFPF have been seen to be about 10 times more fluorescent than C_{60}. Fluorescence spectra of these two derivatives in benzene and benzonitrile are presented in Figure 1B along with that of C_{60} in benzene for comparison. Fluorescence maxima of PPF and PFPF in both of the solvents are blue shifted to ca. 650 nm as compared to that of C_{60} at 725 nm.[63] The fluorescence spectrum of C_{60} has a prominent shoulder at ca. 695 nm. Fluorescence quantum yields (Table 1) have been determined by comparison with that of C_{60} in benzene (1×10^{-4} mol dm^{-3}) as reported in ref 63a. Higher yields of fluorescence for both of the derivatives as compared to that of C_{60} might be a consequence of a lower symmetry of the fullerene derivatives

TABLE 1: Photophysical Properties of C_{60}, PPF, PFPF, and MCPPF

parameters	C_{60}[a,b]	PPF	PFPF	MCPPF[c]
$\lambda_{max}(S_0 \rightarrow S_n)$ nm	231, 257, 329, 440−670	215, 231, 255, 350 (sh), 395 (sh), 460 (sh)	215, 231, 255, 350 (sh), 395 (sh), 460 (sh)	232, 255, 340 (sh), 390 (sh)
λ_{max}(em), nm	740	650	650	
Φ_f	$\sim 1 \times 10^{-4}$	0.7×10^{-3} (BZ) 1.2×10^{-3} (BN)	0.7×10^{-3} (BZ) 0.9×10^{-3} (BN)	
τ_s, ns	1.3 ± 0.1 (BZ)	1.2 ± 0.2 (BZ) 1.9 ± 0.1 (BN)	1.0 ± 0.2 (BZ) 1.5 ± 0.1 (BN)	1.6 ± 0.2 (BZ)
$\lambda_{max}(S_1 \rightarrow S_n)$, nm ($\epsilon$, $dm^3\,mol^{-1}\,cm^{-1}$)[a]	480 (3000), 880 (6300)	610 (3100 ± 1000) 900 (7300 ± 1000)	610 (3200 ± 1000) 900 (7250 ± 1000)	600, 880 (9000 ± 1000)
$\lambda_{max}(T_1 \grave{a} T_n)$, nm ($\epsilon$, $dm^3\,mol^{-1}\,cm^{-1}$)[a]	510 (3000), 740 (14000)	650 (14500 ± 1000) (BZ) 670 (BN)	650 (13000 ± 1000) 670 (BN)	670 (20000 ± 1000)
Φ_T	0.95 ± 0.05 (BZ)	0.49 ± 0.03 (BZ) 0.45 ± 0.03 (BN)	0.61 ± 0.03 (BZ) 0.63 ± 0.03 (BN)	0.45 ± 0.05 (BZ)
τ_T, μs	260	86 ± 2 (BZ) 112 ± 5 (BN)	95 ± 2 (BZ) 150 ± 5 (BN)	110
k_{TS}, $dm^3\,mol^{-1}\,s^{-1}$	2.0×10^8 [a]	$2.3 \pm 0.3 \times 10^8$ (BZ)	$1.2 \pm 0.3 \times 10^8$ (BZ)	5.8×10^8 (BZ)
k_{TT}, $dm^3\,mol^{-1}\,s^{-1}$	1.8×10^9 [a]	8.0×10^9 (BZ) 3.2×10^{10} (BN)	7.0×10^9 (BZ) 1.2×10^{10} (BN)	6×10^9 (BZ)

[a] Reference 68. [b] Reference 69. [c] Reference 57.

and also, in benzonitrile, much stronger interactions with the solvent molecules, which perturb the electronic structure of the fullerene molecule.

B. Laser Flash Photolysis Study. Figure 2 presents the transient absorption spectra obtained on laser flash photolysis of N_2 saturated solution of PPF and PFPF in benzene and benzonitrile, recorded immediately and at 6 ns after the 35 ps laser pulses of 355 nm (energy fluence 2 mJ cm^{-2}). The absorption spectra recorded immediately after the laser pulse show two very broad absorption bands, one in the 500−720 nm region centerd at ca. 600 nm and another in 720−930 nm region with a peak at 900 nm in benzene and 890 nm in benzonitrile. The growth of the transient absorption monitored at 900 nm was observed to follow the rise of the excitation pulse profile in both cases and hence the transient absorption spectra can be assigned to the singlet → singlet ($S_1 \rightarrow S_n$) absorption. Also the lifetimes of the S_1 states have been determined by monitoring the decay of the transient absorption at the same wavelength and have been found to be 1.2 ± 0.2 and 1.9 ± 0.2 ns for PPF and 1.0 ± 0.2 ns and 1.5 ± 0.2 ns for PFPF in benzene and benzonitrile, respectively. The band having a peak at 513 nm in the $S_1 \rightarrow S_n$ absorption spectrum of C_{60} is relatively sharp compared to that having the center wavelength at ca. 600 nm observed for these derivatives (Figure 2a). In addition, the ratio of the absorbance values measured at 890 nm to that at 610 nm in the $S_1 \rightarrow S_n$ spectra of PPF and PFPF are much higher when compared to the ratio of the absorbance at 890 nm to that at 513 nm in the $S_1 \rightarrow S_n$ spectra of C_{60}.[10−13] The transient absorption spectra recorded at 6 ns after the laser pulse can be provisionally assigned to the triplet states of PPF (^{3}PPF*) and PFPF (^{3}PFPF*), formed due to an intersystem crossing (ISC) process from the singlet to the triplet. The spectra have single bands with peaks at 650 and 670 nm in benzene and benzonitrile, respectively, in addition to shoulders at ca. 570 and 700 nm. The transient absorption characteristics are more or less similar in the two solvents studied here. Also, the singlet−singlet and triplet−triplet absorption spectra and the lifetimes of the singlet states of both the derivatives as determined by ps laser flash photolysis are very similar.

The molar extinction coefficient values for the $S_1 \rightarrow S_n$ absorption of PPF and PFPF in benzene has been determined by comparing the absorbance values of the singlet states measured at 900 nm with that of the benzophenone triplet (ϵ (525 nm) = 6500 $dm^3\,mol^{-1}\,cm^{-1}$ in acetonitrile)[59] produced by photoexcitation of the solution with the same ground-state absorption as those of the fullerenes at 355 nm. Under these conditions the molar extinction coefficient values for the excited singlet states of PPF and PFPF in benzene have been determined to be 7300 ± 1000 and 7250 ± 1000 $dm^3\,mol^{-1}\,cm^{-1}$ at 900 nm.

Figure 3A shows the transient optical absorption spectra obtained by laser flash photolysis of N_2 saturated solutions of PPF and PFPF in benzene and recorded at 1 μs after the 35 ps laser pulse. Both spectra exhibt an absorption band at 650 nm with shoulders at ca. 570 and 700 nm and increasing absorption at $\lambda < 350$ nm. The transient species were seen to be efficiently quenched by oxygen, and the entire spectrum of each transient species was seen to follow the same decay law (see later).

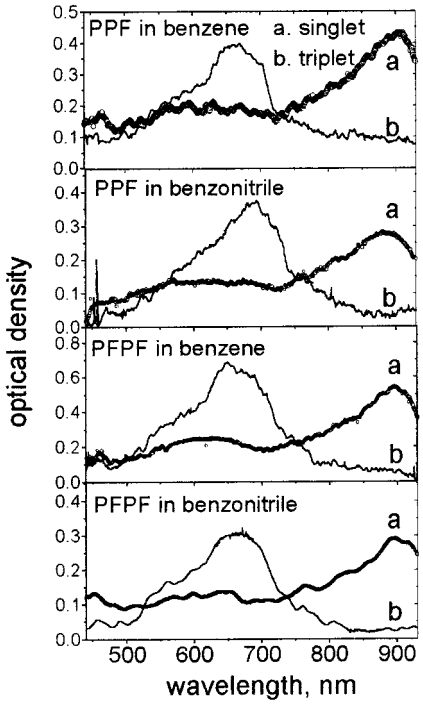

Figure 2. Transient absorption spectra of PPF and PFPF in benzene and benzonitrile, recorded (a) immediately and (b) at 6 ns after the 35 ps laser pulses, respectively.

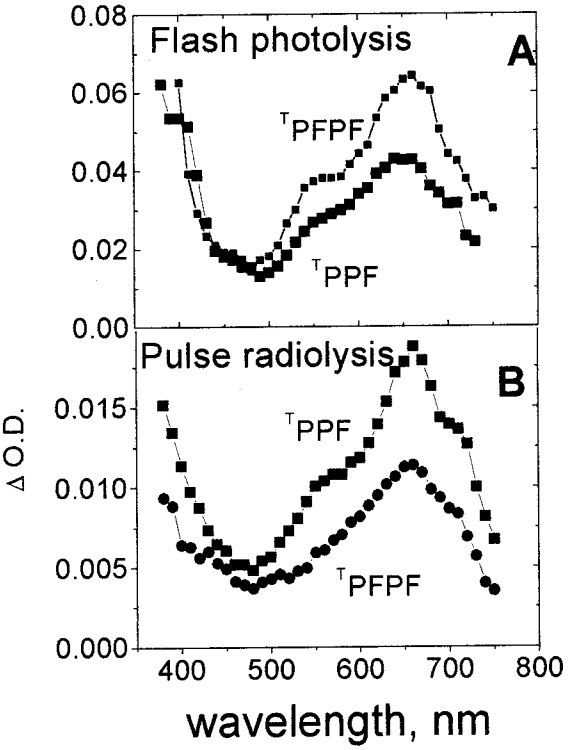

Figure 3. (A) Triplet−triplet absorption spectra of PPF (a) and PFPF (b) in benzene recorded at 1 μs after the laser excitation. (B) Transient optical absorption spectra obtained on pulse radiolysis of N_2-saturated solution of PPF (a) and PFPF (b) in benzene.

Hence, both the spectra can be assigned to a single transient species. They are seen to be very similar to those obtained by ps laser flash photolysis (Figure 2) and therefore can be assigned to the triplet−triplet ($T_1 \rightarrow T_n$) absorption spectra of these fullerene derivatives.

C. Pulse Radiolysis Study. The radiolysis of nonpolar substances such as aliphatic, alicyclic, and also halo-alkanes yields parent and free ions which can be easily used for the time-resolved study of electron transfer processes. In contrast, because of the extremely high mobility of the primarily formed ions in benzene, singlet and triplet excited states dominate. Hence, in the pulse radiolysis of benzene containing a relatively higher concentration ($\sim 10^{-3}$ mol dm^{-3}) of scavenger species, the benzene triplet can serve as a sensitizer for initiating the triplet−triplet energy transfer processes. The radiolysis of benzene produces a triplet of very high energy (353 kJ mol^{-1}) in high yield. The triplet state of benzene can transfer its energy to another solute having E_T < 353 kJ mol^{-1}, thus generating the triplet state of the latter.[64]

$$C_6H_6 \rightarrow {}^3(C_6H_6)^* \quad (1)$$

$$^3(C_6H_6)^* + \text{PPF or PFPF} \rightarrow {}^3(\text{PPF or PFPF})^* + C_6H_6 \quad (2)$$

Conclusive evidence for the assignment of the photolytically generated transient species to the triplet state has been obtained from the pulse radiolysis studies of these solutes in N_2-saturated solutions in benzene.[64] The bimolecular rate constants for energy transfer from the benzene triplet to ^{3}PPF* and ^{3}PFPF* have been determined to be $1.7 \pm 0.05 \times 10^{10}$ and $1.6 \pm 0.05 \times 10^{10}$ dm^3 mol^{-1}s^{-1}, respectively.

Figure 3B shows the transient optical absorption spectra obtained on pulse radiolysis of N_2-saturated solutions of PPF and PFPF (5×10^{-4} mol dm^{-3}) in benzene. An absorption band with λ_{max} at 650 nm with shoulders at 570 and 700 nm was observed for both of the fullerene derivatives. In each case the entire spectrum decayed by first-order kinetics with the rate constants 5.2×10^4 and 4.1×10^4 s^{-1} for PPF and PFPF, respectively. Hence, these spectra can be conclusively assigned to the triplet excited states of PPF and PFPF and are very similiar to those presented in Figure 3A.

The extinction coefficient values for ($T_1 \rightarrow T_n$) absorption (ϵ_T) have been determined by energy transfer from a known triplet which has already been well characterized.[64,65] The energy transfer processes, from the triplet states of the donors (having higher triplet energies than those of the fullerene derivatives), namely, *p*-terphenyl (λ_{max} = 460 nm, ϵ_T = 90 000 dm^3 mol^{-1} cm^{-1}, E_T = 244 kJ mol^{-1}) and biphenyl (λ_{max} = 360 nm, ϵ_T = 27 100 dm^3 mol^{-1} cm^{-1}, E_T = 274 kJ mol^{-1})[65,66] to the fullerene derivatives (the acceptors), have been studied by monitoring the decay of the donor triplets in the presence of the acceptors. The triplets of *p*-terphenyl (^{3}PTP*) and biphenyl (^{3}BP*) were generated on pulse radiolysis of N_2-saturated solutions of PTP and BP in benzene, respectively. The concentration of the donor was kept at 1×10^{-2} mol dm^{-3} and that of the acceptor was varied from $(0-4) \times 10^{-5}$ mol dm^{-3}. Under these conditions, only the triplets of the donor could be produced initially, which in turn transferred energy to the acceptor. The pseudo-first-order decay (k_{obs}) of the ^{3}PTP* was observed to increase linearly with increasing concentration of PPF, suggesting that energy transfer from ^{3}PTP* to ^{3}PPF* has occurred. The energy transfer rate constant was determined from the slope of the linear plot of k_{obs} vs the concentration of PPF, to be $3.1 \pm 0.2 \times 10^9$ dm^3 mol^{-1} s^{-1}. The growth of the transient absorption was also observed at λ = 650 nm simultaneous with the faster decay of ^{3}PTP*. The bimolecular rate constant determined from the growth of the transient absorption at 650 nm gave a value of $4.3 \pm 0.2 \times 10^9$ dm^3 mol^{-1} s^{-1}, close to that determined from the decay of ^{3}PTP* decay. Time-resolved studies showed transient optical absorption spectra similar to that shown in Figure 3, thus confirming the formation of ^{3}PPF*. The molar absorptivity of the $T_1 \rightarrow T_n$ absorption of PPF determined using the method suggested by Amouyal[67] was found to be 13 900 dm^3 mol^{-1} cm^{-1}. The energy transfer rate constant from ^{3}BP to PPF* was also determined in a similar way by monitoring the decay at 360 nm, and the value was found to be 8.6×10^9 dm^3 mol^{-1} s^{-1}. The molar absorptivity of ^{3}PPF* at 650 nm was determined to be 15 200 dm^3 mol^{-1} cm^{-1}, close to the value determined from *p*-terphenyl triplet decay. The average value of the molar absorptivity at 650 nm was calculated to be 14 500 ± 1000 dm^3 mol^{-1} cm^{-1} (Table 1). The studies of energy transfer from ^{3}PTP* and ^{3}BP* to ^{3}PFPF* have also been carried out, and the energy transfer rate constant values have been found to be 1.7×10^9 and 6.1×10^9 dm^3 mol^{-1} s^{-1}, respectively, and the average value of the extinction coefficient for T−T absorption of ^{3}PFPF* be 13000 ± 1000 dm^3 mol^{-1} cm^{-1}.

D. Quantum Yield of Triplet Formation. Using the extinction coefficient values for the excited singlet and triplet absorptions of PPF and PFPF at 900 and 660 nm, respectively, the quantum yields of triplet formation have been calculated to be 0.49 ± 0.03 and 0.61 ± 0.03 in benzene by comparing the absorbance values of the singlet (at 0 ps) and the triplet (at 6 ns) at these two wavelengths (see Figure 2). Similarly, the quantum yields of the triplet formation of PPF and PFPF in benzonitrile have been determined to be 0.45 ± 0.03 and 0.63 ± 0.03 in these two solvents (Table 1), assuming that the extinction coefficient values are the same in benzene and benzonitrle within experimental errors.

E. Decay Kinetics of the Triplet States. It was observed that the decay kinetics of the photolytically generated triplets of PPF and PFPF followed good first-order kinetics in both solvents, benzene and benzonitrile, when the initial concentrations of the triplets produced were very low ($\sim 10^{-6}$ mol dm^{-3}, obtained using lower excitation energy fluence ($\sim$0.1 mJ cm^{-2}) and at low concentrations of the solutes ($\sim 2 \times 10^{-6}$ mol dm^{-3}). However, the decay kinetics of the triplets were not purely single exponential when the higher concentrations of the triplets were initially produced ($\sim 10^{-5}$ mol dm^{-3} obtained using higher excitation energy (3 mJ cm^{-2}) and/or higher solute concentrations ($\sim 10^{-4}$ mol dm^{-3}). Figure 4A shows two typical decay profiles for ^{3}PPF* in benzonitrile recorded with different laser energy fluences, 3 mJ cm^{-2} and 0.1 mJ cm^{-2} and the concentration of PPF of 1.2×10^{-4} mol dm^{-3}. While the decay profile recorded with lower energy excitation fits perfectly to first-order kinetics, the one recorded with higher energy fluence deviates considerably from first-order kinetics and in contrast the decay was observed to follow mixed order kinetics (one component of the decay was seen to follow the second-order kinetics and the other one first order). Hence, it is expected that, in addition to the normal first-order decay of the triplet to the ground state, other possible processes contributing to the decay might include the triplet−triplet annihilation and quenching of the triplet by the ground state.[46,57,68]

To determine the rate constants associated with these processes the decay kinetics of the triplet states were followed using different concentrations of the fullerene derivatives varying from 1.5×10^{-4} mol dm^{-3} to 2.2×10^{-6} mol dm^{-3} as well as with differnt laser energy fluences varying from 3 mJ cm^{-2} to 0.1 mJ cm^{-2}. Each of the decay curves was fitted with the kinetic rate expression as given by eq 3 below.

$$\text{O.D.}\,(t) = \frac{k_1 A_0 \exp(-k_1 t)}{k_1 + k_2 A_0[1 - \exp(-k_1 t)]} \tag{3}$$

$$k_1 = k_T + k_{TS}[\text{Fullerene}] \tag{4}$$

$$k_{TT} = \frac{k_2 \epsilon_T}{A_0} \tag{5}$$

One of the two components which follows first- or pseudo first-order kinetics has been found to be dependent on the concentration of the solute and is related to the self-quenching rate constant (k_{TS}) for the reaction of the triplet with the ground-state molecules and the intrinsic decay rate of the triplet ($k_T = \tau_T^{-1}$) (eq 4). The other component following the second-order kinetics arises due to the T − T annihilation reaction which is prominent at relatively higher concentration of the initially produced triplet and the rate constant (k_{TT}) may be determined using the fitted parameter k_2 following eq 5. The values of k_{TT} were thus determined by fitting the decay profiles recorded with either higher excitation energy or using higher concentration of the solutes to eq 3. The average values obtained from several measurements are given in Table 1.

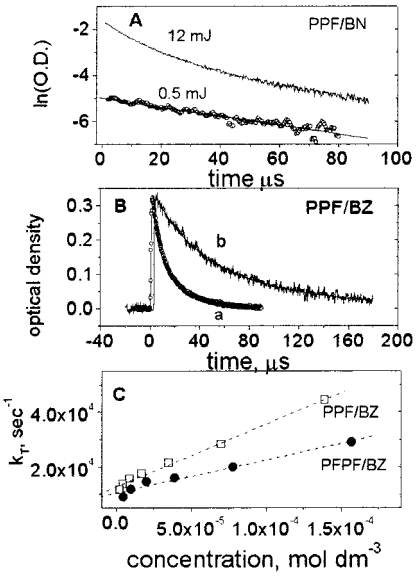

Figure 4. (A) Effect of intensity on the decay kinetics of the ^{3}PPF* in benzonitrile. The decay profiles were recorded with laser energy fluence values of (a) 4 mJ cm^{-2} and 0.4 mJ cm^{-2}. (Concentration of PPF was kept fixed at 1.7×10^{-5} mol dm^{-3}.) (B) Kinetic traces recorded for the decay of ^{3}PPF* in BZ with PPF concentrations of (a) 1.4×10^{-4} mol dm^{-3} and (b) 2.2×10^{-6} mol dm^{-3}. (C) Effect of concentration of PPF and PFPF on their triplet lifetimes (laser energy fluence used were 0.8 mJ cm^{-2}).

The self-quenching rate constants (k_{TS}), for ^{3}PPF* and ^{3}PFPF* in benzene have been determined by monitoring the decay of the triplet species at 650 nm for various concentrations of PPF (2.0×10^{-6} to 1.5×10^{-4} mol dm^{-3}) using the same laser energy fluence (0.8 mJ cm^{-2}) for excitation. The pseudo first-order rate constants for the triplet decay (k_1) decreased from 4.6×10^4 s^{-1} to 1.2×10^4 s^{-1} in the case of ^{3}PPF* and from 2.9×10^4 s^{-1} to 8.9×10^3 s^{-1} in the case of ^{3}PFPF*, while the solute concentration was reduced from 1.5×10^{-4} to 2.2×10^{-6} mol dm^{-3}. Decay traces presented in Figure 4B show the variation of the lifetimes of the ^{3}PPF* at the two extreme concentration conditions along with the fit functions obtained using eq 3. Figure 4C shows the plots of these k_1 values against the concentrations of the fullerenes used. The self-quenching rate constants (k_{TS}) and the actual triplet lifetimes ($\tau_T = k_T^{-1}$) calculated from the slope and intercept of the least-squares fit lines (eq 4) are presented in Table 1.

F. Charge Transfer Interaction with DPA and TPA. *Steady-State Studies.* The optical absorption spectra of PPF and PFPF ($\sim 1 \times 10^{-4}$ mol dm^{-3}) in benzonitrile solutions showed

TABLE 2: Electron Transfer Properties of PPF and PFPF

acceptor	donor	K_{CT}, dm^3 mol^{-1}	ϵ_{CT} (600 nm) dm^3 mol^{-1} cm^{-1}	donor conc (mol dm^{-3})	$\tau_{singlet}$, ps (890 nm)	τ_{cation}, ps (700 nm/660 nm)	k_{ET}, 10^{10} dm^3 mol^{-1} s^{-1}	k_{BET}, 10^{10} dm^3 mol^{-1} sec^{-1}
PPF	DPA	0.75	350	0	1900		1.27	11.2 ± 0.3
				0.3	410	670		
				0.6	120	350		
				0.9	80	270		
	TPA			0	1900		1.16	6.3 ± 0.3
				0.3	390			
				0.6	122			
PFPF	DPA	2.3	360	0	1500		1.10	22.5 ± 0.5
				0.3	540	740		
				0.6	140	400		
				0.9	100	340		

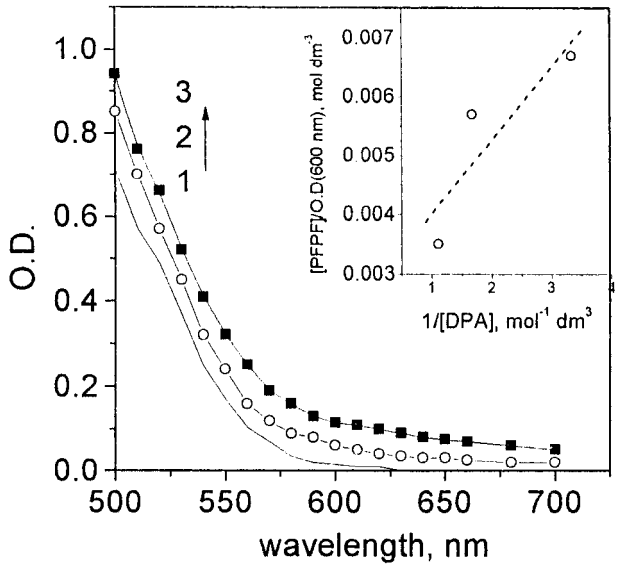

Figure 5. Change in absorption spectra of PFPF in benzonitrile in the presence of different concentrations of DPA due to CT complex formation ([DPA] = (1) 0; (2) 0.3, and (3) 0.9 mol dm^{-3}). Inset: The Benesi−Hildebrand plot for PFPF−DPA CT complex, assuming 1:1 association between the two.

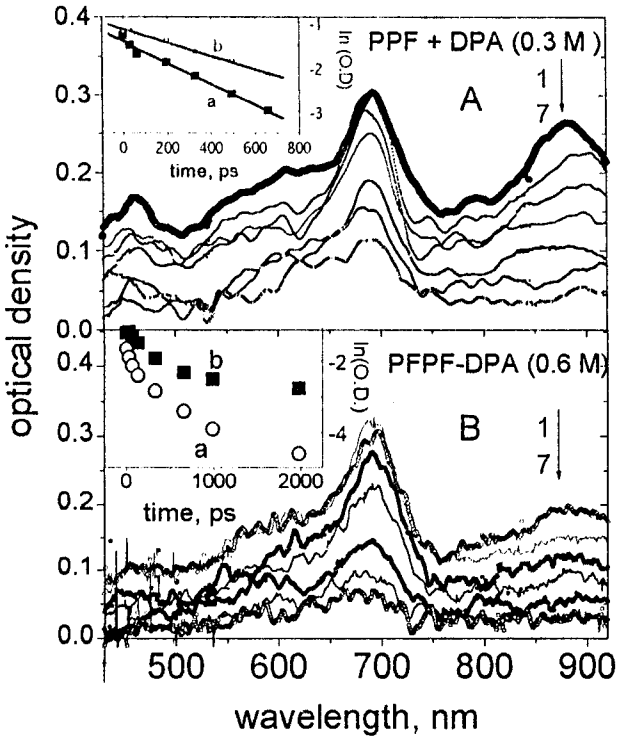

Figure 6. Time-resolved transient absorption spectra obtained on 532 nm excitation of the solutions containing (A) PPF and 0.3 mol dm^{-3} of DPA (time delays: (1) 0; (2) 33; (3) 66; (4) 132; (5) 330; (6) 495, and (7) 660 ps) and (B) PFPF and 0.6 mol dm^{-3} of DPA (time delays: (1) 0; (2) 33; (3) 66; (4) 132; (5) 330; (6) 660, and (7) 1980 ps) in benzonitrile. Insets show the first-order plots for the decay of (a) ^{1}PPF* or ^{1}PFPF* and (b) DPA$^{\bullet+}$ measured at 890 and 700 nm, respectively.

increased absorption in the 500−700 nm wavelength region on gradual addition of DPA or TPA. These amines in benzonitrile have very little absorption above 400 nm. Hence, the increased absorption on addition of amines may possibly be due to the formation of charge transfer complexes (CT) between the fullerene derivatives and the amines in the ground state. Similiar observations have already been made in the case of C_{60} and its other derivatives, which have high electron affinities (2.6−2.8 eV) and have been shown to form CT complexes with electron-rich amines in the ground state.[69,70] Figure 5 shows the change in absorption spectra of PFPF in benzonitrile in the presence of different amounts of DPA due to formation of CT complex in the ground state. However, no indication for the ground state CT complex formation between PPF or PFPF with DPA or TPA in benzene has been obtained probably due to the low polarity of the solvent, which does not favor the charge transfer interaction.

Considering the formation of a 1:1 complex in the ground state (eq 6), the values for the molar extinction coefficient (ϵ_{CT}) and the equilibrium constant (K_{CT}) for the CT complex have been determined by applying the Benesi−Hildebrand equation (eq 7).[71] The inset of Figure 5 shows a typical Benesi−Hildebrand (B−H) plot for PFPF-DPA complex. The linear nature of the B−H plot indicates the formation of a 1:1 complex.

$$\text{fullerene} + \text{amine} \rightarrow [\text{fullerene}^{\delta-} \cdots \text{amine}^{\delta+}] \qquad (6)$$

$$\frac{[\text{fullerene}]}{\text{O.D.}_{600\ \text{nm}}} = \frac{1}{K\epsilon_{CT}[\text{amine}]} + \frac{1}{\epsilon_{CT}} \qquad (7)$$

The values of ϵ_{CT} and K_{CT} for the PPF-DPA and PFPF-DPA pairs are given in Table 2. Due to very low extinction coefficient values of the CT compexes at 600 nm, the error limit in determination of k_{CT} values are quite high (say about 20%). Despite that the fullerenes are big molecules and capable of providing more than a few sites for attachment of the small amine molecules, the formation of CT complex of only 1:1 composition is a bit surprising. From the equilibrium constant values it can be estimated that about 90% or more of the PPF or PFPF molecules are involved in complex formation when the amine concentration is about 0.9 mol dm^{-3}.

Time-Resolved Studies. The dynamics of charge transfer in the excited CT complex as well as in the excited singlet state have been investigated by ps laser flash photolysis on excitation at 532 nm. Excitation of the solutions containing the fullerene derivatives and the amines in benzonitrile by this light does not excite the amines but does the CT complex as well as the free fullerene molecules present in solution. Also, biphotonic ionization of these amines could be avoided by keeping the laser energy fluence low (less than 1.6 mJ cm^{-2}). Blank experiments with the solutions containing only amines in benzonitrile were also performed under similar conditions to ensure that the cation radicals were not formed via biphotonic ionization of the amines.

Figure 6A shows the time-resolved transient absorption spectra obtained on ps laser flash photolysis of the solution containing PPF and 0.3 mol dm^{-3} of DPA in benzonitrile. The spectrum recorded immediately after the laser pulse (curve 1) was seen to be different from that obtained on laser flash photolysis of only PPF in benzonitrile solution (Figure 2). The former has two distinct bands with maxima at ca. 700 and 890 nm. The transient absorbance at 890 nm was seen to follow first-order kinetics with a lifetime of 410 ± 25 ps (curve a in inset of Figure 6A). This lifetime value is much shorter than the lifetime (1.9 ns) of the singlet state of PPF in benzonitrile (Table 1). The 890 nm band probably can be assigned to ^{1}PPF* which has been formed due to direct excitation of free PPF (not involved in complexation) in solution and quenched by DPA. The band with a peak at 700 nm could be assigned to the cation radical of DPA (DPA$^{\bullet+}$)[8,9,72] in a singlet ion pair (IP) formed due to charge separation in the excited CT complex (Scheme 2). An absorption maximum of free DPA$^{\bullet+}$ in polar solvents

has been reported to appear at 670 nm.[73,74] But in our earlier studies[9,57,72] we observed the maximum due to $DPA^{\bullet+}$ present in the fullerene−amine ion pair to appear at 700 or 710 nm. $^3PPF^*$ in benzonitrile has the absorption peak at 670 nm but the peak of the transient observed here is at 700 nm and also the width of the band is much narrower than that of the triplet state spectrum (Figure 2). Hence, the absorption peak observed at 700 nm is definitely not due to $^3PPF^*$ but may be assigned to $DPA^{\bullet+}$, formed due to charge separation in the excited state of the CT complex. Absorption due to $DPA^{\bullet+}$ was observed to remain constant up to 33 ps and then to decrease gradually with time (curve b in inset of Figure 6). The initial growth of absorption at 700 nm is possibly due to formation of $DPA^{\bullet+}$, either via diffusional electron transfer quenching of $^1PPF^*$ by free DPA remaining in the solution or by charge separation in the excited CT complex (see later for discussion). The decrease of absorption of the cation radical later can be assigned to geminate recombination in the singlet ion-pair with the counter radical anion ($PPF^{\bullet-}$), which probably has a very small absorption coefficient below 930 nm. We could not detect any transient absorption with this solution beyond 2 ns time delay The geminate recombination rate measured by monitoring the decay of the transient absorption at 700 nm has been found to be 670 ps. Since the pseudo first-order rate of electron transfer reaction between $^1PPF^*$ and DPA ($k_{et} = \tau_s^{-1} = 2.4 \times 10^9\ s^{-1}$) is about more than five times faster than that of the ISC process ($k_{ISC} \sim 5.3 \times 10^8\ s^{-1}$), the formation of $^3PPF^*$ via the ISC process from $^1PPF^*$ should not be able to compete with the former one. Hence, the contribution of the triplet toward the transient absorption decay monitored at 700 nm can be neglected, and the geminate recombination in the ion pair might be considered as the major process responsible for the transient decay monitored at 700 nm.

The same experiment was repeated with the higher concentrations of DPA, i.e., 0.6 and 0.9 mol dm^{-3} of DPA. Although the decay profiles of both $^1PPF^*$ as well as $DPA^{\bullet+}$ monitored at 890 and 700 nm, respectively, showed exponential decay behavior while the concentration of DPA used was kept low (<0.6 mol dm^{-3}), the decay kinetics showed a deviation from the linear behavior in solutions with higher concentrations of DPA (see later). The average lifetime values thus obtained from monoexponential fittings have been provided in Table 2. With these concentrations of DPA the lifetimes for $^1PPF^*$ were determined to be 120 and 80 ps, respectively. Hence, it is seen that the dynamic quenching rate of $^1PPF^*$ is increased due to an increase in concentration of DPA. The dynamic quenching rate constant determined from the Stern−Volmer (S−V) plot is $1.27 \pm 0.05 \times 10^{10}$ $dm^3\ mol^{-1}\ sec^{-1}$, which is near the diffusion controlled rate constant in benzonitrile. This should be the rate constant for electron transfer reaction (k_{ET}) between $^1PPF^*$ and DPA via diffusional encounter. Table 2 shows that the geminate recombination rate determined by following the decay of the transient absorption of $DPA^{\bullet+}$ at 700 nm increases with increase in concentration of DPA in solution.

Figure 6B shows the time-resolved absorption spectra of the transient produced due to laser flash photolysis of a solution containing PFPF and 0.6 mol dm^{-3} of DPA in benzonitrile. The spectrum recorded at 0 ps shows two major peaks at 700 and 890 nm. The absorbance monitored at 700 nm shows a growth for the first 33 ps and then starts decaying. The decay dynamics of both $DPA^{\bullet+}$ and $^1PFPF^*$ monitored at 700 and 890 nm showed nonexponential behavior with average lifetimes of 400 and 140 ps, respectively. In addition, the peak appearing at 700 nm at zero ps time delay has been seen to shift gradually to 670 nm after 1.8 ns. However, the ISC process from $^1PFPF^*$ can be considered to be negligible in this case too. These facts indicate that the decay behavior of $DPA^{\bullet+}$ is quite complicated and possibly more than one species, e.g., different kinds of IPs and/or free $DPA^{\bullet+}$, might be responsible for the decay dynamics monitored at 700 nm (see later). The decay lifetimes of $^1PFPF^*$ measured with other two concentrations of DPA (e.g., 0.3 and 0.9 mol dm^{-3}) are given in Table 2. The k_{ET} value for the interaction between $^1PFPF^*$ and DPA determined from the Stern−Volmer plot has been found to be $1.10 \pm 0.05 \times 10^{10}$ $dm^3\ mol^{-1}\ s^{-1}$. The geminate recombination rates as seen from Table 2 also increase with increase in concentration of $DPA^{\bullet+}$ produced initially in experiments using higher concentrations of DPA. However, the nonexponential decay kinetics observed at 890 nm at higher concentrations of the amines possibly indicates the presence of another species. This might be the anion radical of the fullerene derivative, which has a small absorption coefficient in this wavelength region.[75] The anion radical in the ion pair is also involved in the geminate recombination process.

Hence, it has been evident from the above discussion that the decay dynamics of the cation radical, $DPA^{\bullet+}$ monitored at 700 nm show nonexponential behavior and need discussion. Mataga and co-workers[76] have examined the photoinduced charge separation (CS) and charge recombination (CR) reactions in tetracyaonenzene (TCNB)−toluene CT complexes in acetonitrile. Their results indicate that the solvent reorientation can induce CS to a considerable extent within a few ps but not completely. For complete CS leading to ion pair (IP) formation, further intracomplex structural change and solvation, which take about a few tens of ps, appears to be necessary. The initial growth of $DPA^{\bullet+}$ up to about 33 ps might be due to either of two reasons. One of them might be due to quenching of the excited singlet state of the fullerene derivative ($^1F^*$) by DPA via ET reaction. Using this rate constant, $k_{ET} \sim 1.2 \times 10^{10}$ $dm^3\ mol^{-1}\ s^{-1}$ (Table 2) and the concentration of the amine used, which is about 0.5 mol dm^{-3}, the lifetime of the growth of $DPA^{\bullet+}$ can be calculated to be about 170 ps. Hence, this process cannot be responsible for the growth of $DPA^{\bullet+}$. The other process is the charge separation (CS) and solvent relaxation in the excited CT complex leading to an ion pair having an absorption maximum at 700 nm, and possibly they are responsible for the initial growth of absorption of $DPA^{\bullet+}$.

The IP formed by exciting the CT complex may have a tighter structure with stronger interaction between the donor and the acceptor radical ions in the pair than in the IP produced by CS at the encounter between the excited acceptor and the donor. The decay dynamics and the chemical reactivity of the IP formed by excitation of the CT complex should be quite different from that of the IP produced by the CS through an encounter between $^1F^*$ and the amine. The IP produced by CT complex excitation will be the contact ion pair (CIP) without intervening solvent molecules between the donor and acceptor radical ions in the pair. The IP formed by interaction between $^1F^*$ and the amine by diffusional encounter will be the so-called solvent separated ion pair (SSIP) with the solvent molecules intercepted between the donor and the acceptor radical ions. As a consequence of these structural differences there should be a much stronger interaction between the geminate radical ion pairs in the CIP, which results in remarkably higher k_{CR} values compared with those of the ion pairs in SSIP. Also, we discussed earlier that although the absorption maximum of $DPA^{\bullet+}$ in singlet ion pair appeared at 700 nm at zero delay, at later time the band due to $DPA^{\bullet+}$ broadened and a peak at 670 nm appeared. This probably

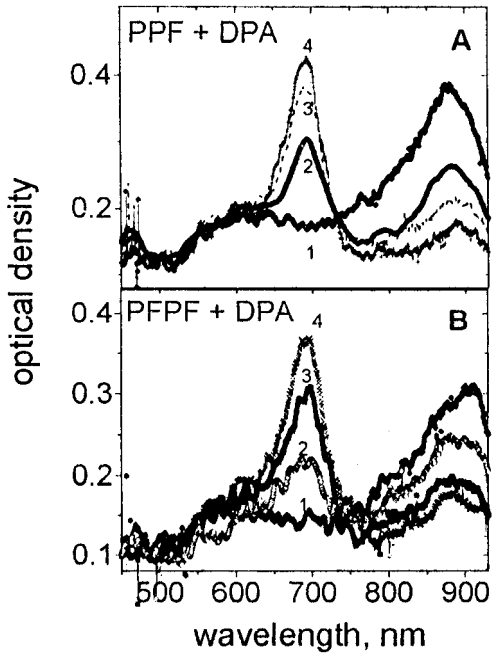

Figure 7. Transient absorption spectra recorded immediately after the laser pulse excitation of the solution containing (A) PPF or (B) PFPF and different concentrations of DPA [(1) 0; (2) 0.3; (3) 0.6; and (4) 0.9 mol dm^{-3}] in benzonitrile.

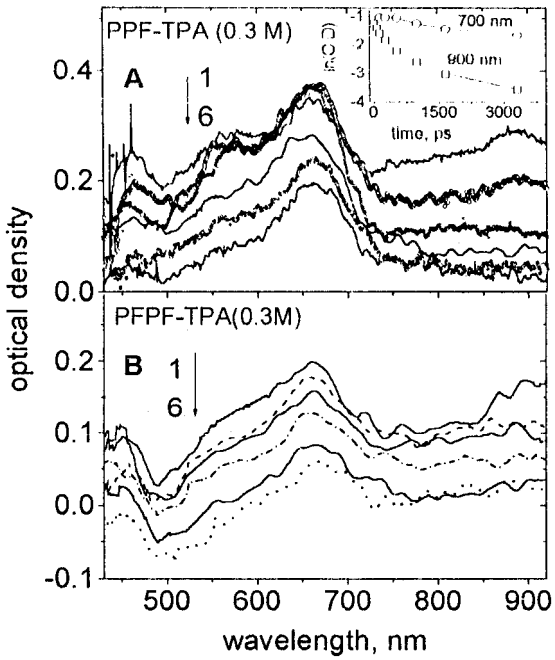

Figure 8. Time-resolved transient absorption spectra obtained on 532 nm excitation of the solutions containing (A) PPF and 0.3 mol dm^{-3} of TPA (time delays: (1) 0; (2) 0.13; (3) 0.5; (4) 0.99; (5) 1.65; and (6) 5 ns) and (B) PFPF and 0.3 mol dm^{-3} of DPA (time delays: (1) 0; (2) 0.33; (3) 0.5; (4) 1.98; (5) 3.33; and (6) 5 ns) in benzonitrile. Inset shows the first-order plots for the decay of (a) ^{1}PPF* and (b) $TPA^{\bullet+}$ measured at 890 and 660 nm, respectively.

indicates the formation of SSIP and/or free $DPA^{\bullet+}$, which escape geminate recombination in ion pair. Both of these species undergo back electron transfer (BET) reaction at longer time. These facts probably explain the nonexponential character of the decay dynamics of $DPA^{\bullet+}$ monitored at 700 nm and indicate the presence of two kinds of ion pairs, namely, CIP and SSIP, as well as free $DPA^{\bullet+}$. The formation of free $DPA^{\bullet+}$ is possibly a very minor channel and the major decay channel for both kinds of ion-pairs is the geminate recombination. The formation of CIP in high concentration probably explains the faster geminate recombination rate measured in the presence of higher concentrations of the donors.

Figure 7 shows the transient absorption spectra obtained immediately after 35 ps laser pulses following photolysis of the three solutions containing PPF (or PFPF) and three different concentrations of DPA (0.3, 0.6, and 0.9 mol dm^{-3}). It is observed that the concentrations of ^{1}PPF* produced at zero time delay due to direct excitation of free PPF are decreased because of a decrease in concentration of free PPF present in the solutions due to formation of CT complex between DPA and PPF (or PFPF) in the ground state. Also, the decrease in absorption at 890 nm with increase in concentration of the donors is indicative of the fact that the anion radicals ($PPF^{\bullet-}$ and $PFPF^{\bullet-}$) have very small or negligible absorption in this wavelength region. Hence, the bands observed at 890 nm with the lower concentrations of the donors are mainly due to the excited singlet state produced as a result of direct excitation of the residual uncomplexed fullerene molecules. Also, the decay lifetimes monitored at 890 nm are different from those of the cation radicals monitored at 700 nm, and this fact indicates the interaction of the excited singlet state with the free amines in solution by diffusional encounter.

Figure 8 presents the time-resolved transient absorption spectra obtained due to laser photolysis of PPF (A) and PFPF (B) in the presence of 0.3 mol dm^{-3} of TPA in benzonitrile. In each case the absorption peak at 660 nm in the absorption spectra recorded immediately after the 35 ps laser pulse indicates the formation of $TPA^{\bullet+}$ due to charge separation in the excited state of the fullerene−TPA CT complexes. The decay of $TPA^{\bullet+}$ as monitored at 660 nm[9,72] shows nonexponential behavior in both the cases. The average lifetimes of $TPA^{\bullet+}$ (Table 2) in the PPF−TPA system have been found to be longer in the presence of higher concentrations of TPA, and no meaningful explanation could be provided here. Probably this fact indicates the formation of some kind of degradation products since the steady-state absorption spectra of the solutions after the photolysis experiments were seen to be quite different from the original solution. In the presence of 0.3 and 0.6 mol dm^{-3} of TPA, the lifetimes of ^{1}PPF* were determined to be 390 and 122 ps (Table 2) by measuring the absorbance decay at 900 nm. This indicates that the quenching of ^{1}PPF* occurs by electron transfer in diffusional encounters with free TPA in solution, and this rate has been determined to be 1.16×10^{10} dm^3 mol^{-1} cm^{-1}. However, in the case of PFPF the same result remains inconclusive because the lifetime determined was longer than that of ^{1}PFPF*. This fact may indicate some product formation between PFPF derivative and amine. Moreover, this is also indicated by the negative absorption growing at 500 nm with time (Figure 8B).

To investigate the interaction between the triplet states of these fullerene derivatives with the amines, the laser flash photolysis study in the nano and microsecond time domain was performed in the presence of very low concentrations ($\sim 10^{-3}$ mol dm^{-3}) of the amines in benzonitrile. Figure 9 shows the time-resolved transient absorption spectra obtained due to photolysis of PPF and PFPF ($\sim 1 \times 10^{-5}$ mol dm^{-3}) in benzonitrile in the presence of 2.5×10^{-3} mol dm^{-3} of DPA (A) and TPA (B). No indication of CT complex formation in the ground state has been obtained at such low concentration of the donors. The spectra recorded at 1 μs after the laser pulse have been seen to be very broad with peaks at ca. 670 nm for both of the fullerenes. Due to the close proximity of the maxima of the triplet absorption to that of $DPA^{\bullet+}$ or $TPA^{\bullet+}$, the decay

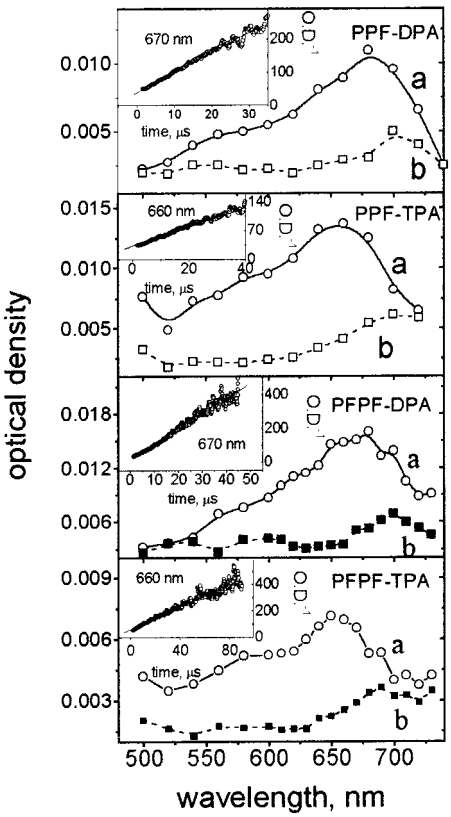

Figure 9. Transient absorption spectra obtained on photolysis of PPF and PFPF in the presence of 2.5×10^{-2} mol dm^{-3} of DPA or TPA in benzonitrile by 355 nm laser pulses of 35 ps duration and 1.5 mJ cm^{-2} fluence. Inset shows the second-order plot for the decay profile measured at 660 nm.

and formation kinetics of these species could not be followed accurately. However, the perfect second-order decay kinetics measured at 660 or 670 nm (insets of Figure 9) indicates the formation of amine cation radicals. We have already mentioned that there is no CT complex formation in the ground state at such low concentrations of the amines. Also, assuming the diffusion-controlled rate constant in benzonitrile be 3×10^{10} dm^3 mol^{-1} s^{-1} and using the concentration of the amine used be 5×10^{-3} mol dm^{-3}, the diffusion-controlled bimolecular rate, which should be the maximum rate for the interaction between ^{1}F* and the amines, can be calculated to be 7.5×10^8 s^{-1}. This rate is much slower than the deacy rate of the singlet ($k_s = \tau_s^{-1} = 5.26 \times 10^9$ s^{-1}). Hence, the formation of the cation radical due to interaction with the excited singlet state in this case could be ruled out. Therefore, the cation radical must have been formed due to interaction between ^{3}PPF* or ^{3}PFPF* and the amines. The second-order decay of the cation radicals measured at 670 or 660 nm could be assigned to the back electron transfer reaction between the free cation and anion radicals present as SSIP. These rate constant (k_{BET}) values have been given in Table 2. The values of k_{BET}, faster than the diffusion controlled rate in this solvent, indicate that the back electron transfer reactions take place in SSIP, before the radical ions get separated from each other. The absorption spectra recorded at 30 μs after the laser pulse could possibly be attributed to the products formed due to photoinduced chemical reactions between the fullerenes and the amines.

As a result of the preceding facts reaction Scheme 2 can be formulated for the whole events of CS and CR reactions in the present case.

SCHEME 2

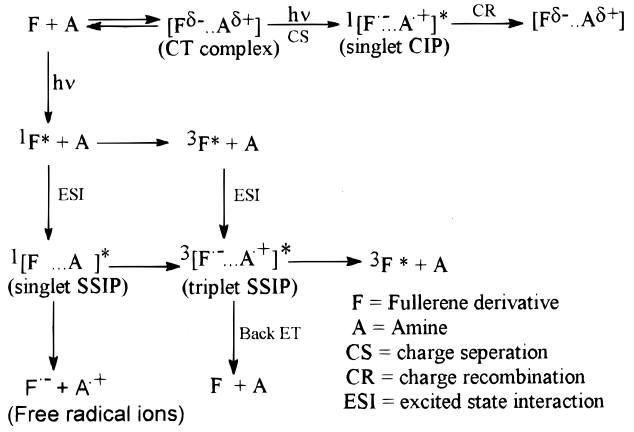

Conclusions

The photophysical properties of the singlet and the triplet states of two aryl-substituted derivatives of C_{60}, reported in this manuscript (Table 1), are closely comparable but are quite different to those of C_{60}. The sharp absorption bands of C_{60}, in the ground state, are broadened by the presence of the functional groups. The lifetimes of the singlet states are nearly the same (ca ~1.5 ns), but the visible band (480 nm) of the C_{60} singlet state shows a red shift to 610 nm in these two derivatives. The near-infrared absorption band (890 nm) remains unchanged. The near-infrared absorption band (740 nm) of the triplet state of C_{60} is blue shifted to ca. 660 or 670 nm in these two derivatives, but the absorption coefficient remains nearly the same. The quantum yields and the lifetimes of the triplet states are shown to decrease on addition of the functional groups to C_{60}. It may therefore be concluded that the photophysical properties of the singlet and triplet states and also of the ground state are significantly affected by the presence of the substituents. However, due to efficient self-quenching and T−T annihilation reactions of the triplets of these derivatives, they are promising nonlinear optical materials and these properties are being investigated presently in our laboratory.

The electron transfer properties of two substituted fullerene derivatives have also been investigated. They form weaker complexes and show weaker charge transfer activities with the aromatic amines. In benzne the interaction is too weak to obtain any indication of complex formation. Hence, the electron transfer reactions for these two fullerene dervatives have been investigated in more polar solvent benzonitrile. However, the electron transfer properties of C_{60} could not be investigated in benzonitrile because of its strong aggregation properties in this solvent[77] and hence could not be compared. By the fact that the present derivatives do not form charge transfer complexes in nonpolar solvent, benzene, while C_{60} interacts strongly with these amines in this solvent, it can be concluded that the former are weaker electron acceptors. No evidence could be obtained regarding aggregation of the fullerene derivatives in either of the solvents.

Acknowledgment. The authors are grateful to Dr. A. V. Sapre of RC&CD, BARC and Prof. D. R. M. Walton of Fullerene Science Centre, University of Sussex, for fruitful discussion on the results.

References and Notes

(1) Tutt, L.; Kost, K. *Nature* **1992**, *356*, 225.

(2) Maggini, M.; Scarrano, G.; Prato, M.; Brusatin, G.; Innocenzi, P.; Guglielmi, M.; Renier, A.; Signorini, R.; Meneghettt, M.; Bozio, R. *Adv. Mater*. **1995**, *7*, 404.

(3) Saricifti, N. S.; Swilowitz, L.; Heagu, A. J.; Wudl, F. *Science* **1992**, *258*, 1474.

(4) Sariafti, N. S.; Heau, A. J. U. S. Patents 5,331,183, 1994 and 5,454,880, 1995.

(5) Richmond, R. S.; Gibbson, U. J. In *Recent Advances in the Chemistry and Physics of Fullerenes and Related Materials*; Kadish, K. M., Ruoff, R. S., Eds. The Electrochemical Society: Pennigton, N. J., 1995; p 684.

(6) Boutorine, A. S.; Tokuyama, H.; Takasugi, M.; Isobe, H.; Nakamura, E.; Helene, C. *Angew. Chem.* **1994**, *23*, 2526.

(7) Hirsch, A. In *The Chemistry of the Fullerenes*; Thieme Medical Publishers Inc.: New York, 1994.

(8) Palit, D. K.; Sapre, A. V.; Mittal, J. P.; Rao, C. N. R. *Chem. Phys. Lett.* **1992**, *195*, 1.

(9) Palit, D. K.; Mittal, J. P. *Fullerene Sci. Technol.* **1995**, *3*, 643.

(10) Sension, R. J.; Phillips, C. M.; Szarka, A. Z.; Romanow, W. J.; McGhie, A. R.; McCauley, J. R.; Smith A. B.; Hochstrasser, R. M. *J. Phys. Chem.* **1991**, *95*, 6075.

(11) Ebbesen, T. W.; Tanigaki, K.; Kuroshima, S. *Chem. Phys. Lett.* **1991**, *181*, 501.

(12) Foote, C. S. *Top. Curr. Chem.* **1994**, *169*, 348.

(13) Anderson, J. L.; An, Y. -Z.; Rubin, Y.; Foote, C. S. *J. Am. Chem. Soc.* **1994**, *116*, 9763.

(14) Irie, K.; Nakamura, Y.; Ohigashi, H.; Tokuyama, H.; Yamago, S.; Nakamura, E. *Biosci. Biotechnol. Biochem.* **1996**, *60*, 1359.

(15) Friedman, S. H.; Decamp, D. L.; Sijbesma, R.; Srdanov, G.; Wudl, F. *J. Am. Chem. Soc.* **1993**, *115*, 6506.

(16) (a) Hebbard, A. F.; Rosseinsky, M. J.; Haddon, R. C.; Murphy, D. W.; Glarum, S. H.; Palstra, T. T. M.; Ramierez, A. P.; Korton, A. R. *Nature* **1991**, *350*, 600. (b) Tanigaki, K.; Ebbesen, T. W.; Sato, J.; Mizuki, J.; Tsai, J. S.; Kubo, Y.; Kuroshima, S. *Nature* **1991**, *352*, 222.

(17) (a) Allemond, P.-K.; Khemani, K. C.; Koch, A.; Wudl, F.; Holezr, K.; Donovan, S.; Gruner, G.; Thompson, J. D. *Science*, **1991**, *253*, 301. (b) Stephens, P. W.; Cox, D.; Hanher, J. W.; Mihaly, L.; Wiley, J. B.; Allemand, P.-K.; Hirsch, A.; Holezer, K.; Li, Q.; Thompson, J. D.; Wudl, F. *Nature* **1992**, *355*, 331.

(18) (a) Wang, Y. *Nature* **1992**, *356*, 585. (b) Wang, Y.; Ynan, C. H. *J. Am. Chem. Soc.* **1993**, *115*, 3844.

(19) Mclean, D. G.; Sutherland, R. L.; Brant, M. C.; Brandelik, D. M. *Opt. Lett.* **1993**, *18*, 858.

(20) Riggs, J. E.; Sun, Y.-P. *J. Phys. Chem. A* **1999**, *103*, 485.

(21) Taylor, R. *J. Chem. Soc., Perkin Trans. 2* **1992**, 1667.

(22) Taylor, R. *Philos. Trans. R. Soc. London A* **1993**, *343*, 87.

(23) Austin, S. J.; Batten, R. C.; Fowler, P. W.; Redmond D. B.; Taylor, R. *J. Chem. Soc., Perkin Trans. 2* **1993**, 1383.

(24) Rathna, A.; Chandrasekhar, J. *Chem. Phys. Lett.* **1993**, *206*, 217.

(25) Dunlop, B. I.; Brenner, D. W.; Schriver, G. W. *J. Phys. Chem.* **1994**, *98*, 8, 4283.

(26) Book, L. D.; Scunseria, G. E. *J. Phys. Chem.* **1994**, *98*, 4283.

(27) Olah, G. A.; Bucsi, I.; Lambert, C. L.; Aniszfeld, R.; Trivedi, R. J.; Sensharma, D. K.; Prakash, G. K. *J. Am. Chem. Soc.* **1991**, *113*, 9385.

(28) Tebbe, F. N.; Becker, J. Y.; Chase, D. B.; Firment, L. E.; Holler, E. R.; Malone, B. S.; Krusic, P. J.; Wasserman, E. J. *J. Am. Soc.* **1991**, *119*, 9900.

(29) Selig, H.; Lifshitz, C.; Peres, T.; Fischer, J. E.; McGhie, A. R.; Romanow, W. J.; McCauley, J. P.; Smith, A. B. *J. Am. Chem. Soc.* **1991**, *113*, 5475.

(30) Birkett, P. R.; Hitchcock, P. B.; Kroto, H. W.; Taylor, R.; Walton, D. R. M. *Nature* **1992**, *357*, 479.

(31) Holloway, J. H.; Hope, E. G.; Taylor, R.; Langley, R.; Avent, A. G.; Dennis, T. J.; Hare, J. P.; Kroto, H. W.; Walton, D. R. M. *J. Chem. Soc., Chem. Commun.* **1991**, 966.

(32) Bausch, J. W.; Prakash, G. K.; Olah, G. A. *J. Am. Chem. Soc.* **1991**, *113*, 3205.

(33) Seshadri, R.; Govindaraj, A.; Nagarajan, R.; Pradeep, T.; Rao, C. N. R. *Tetrahedron Lett.* **1992**, *33*, 2069.

(34) Haufler, R. E.; Conceicao, J.; Chibante, P. F.; Chai, Y.; Byrne, N. E.; Flanagan, S.; Haley, M. M.; O'Brien, S. C.; Pan, C.; Xiao, Z.; Billups, W. E.; Cinufolini, M. A.; Hauge, R. H.; Margrave, J. L.; Wilson, L. J.; Curl R. F.; Smalley, R. E. *J. Phys. Chem.* **1990**, *94*, 8634.

(35) Russ, T. D.; Prato, M. *J. Org. Chem.* **1996**, *61*, 9070.

(36) Lu, Q.; Schestu, D. I.;.Wilson, S. R. *J. Org. Chem.* **1996**, *61*, 4764.

(37) Guldi, D. M.; Asmus, K. D. *J. Phys. Chem. A* **1997**, *101*, 1472.

(38) Lamparth, I.; Hirsch, A. *J. Chem. Soc., Chem. Commun.* **1994**, 1727.

(39) Guldi, D. M.; Hungerbuhler, H.; Asmus, K. D. *J. Phys. Chem. A* **1997**, *101*, 1783.

(40) Guldi, D. M.; Hungerbuhler, H.; Asmus. K. D. *J. Phys. Chem. A* **1995**, *99*, 13487.

(41) Chiang, L. Y.; Swirczewski, J. W.; Hu, C. S.; Chowdhury, S. K.; Cameron, S.; Creegan, K. *J. Chem. Soc., Chem. Commun.* **1992**, 1791.

(42) Chiang, L. Y.; Wang, S. M.; Tseng, S. M.; Hu, J. S.; Hsieh, K.-H. *J. Chem. Commun.* **1994**, 2675.

(43) Maggini, M.; Karlsson, A.; Parimemi, L.; Scorrano, G.; Prato, M.; Vaili, L. *Tetrahedron Lett.* **1994**, *35*, 2985.

(44) Vesella, A.; Uhlmann, P.; Waldraff, C. A.; Diedrich, F.; Thilgen, C. *Angew. Chem., Int. Ed. Engl.* **1992**, *31*, 1388.

(45) Hawker, C.; Saville, P. M.; White, J. W. *J. Org. Chem.* **1994**, *59*, 3503.

(46) Zhang, X.; Foote, C. S. *J. Org. Chem.* **1994**, *59*, 5235.

(47) Maggini, M.; Scorrano, G.; Prato, M. *J. Am. Chem. Soc.* **1993**, *115*, 9798.

(48) Wilson, S. R.; Kaprindis, N.; Wu, Y.; Schuster, D. I. *J. Am. Chem. Soc.* **1993**, *115*, 8495.

(49) Birgel, C. *Chem. Ber.* **1957**, 126.

(50) Hirsch, A.; Lamparth, I.; Karfunkal, H. R. *Angew. Chem., Int. Ed. Engl.* **1994**, *33*, 437.

(51) Guldi, D. M. *J. Phys. Chem. A* **1997**, *101*, 3895.

(52) .Guldi, D. M. *Res. Chem. Intermed.* **1997**, *23*, 653.

(53) Guldi, D. M.; Liu, D.; Kamat, P. V. *J. Phys. Chem. A* **1997**, *101*, 6195.

(54) Kamat, P. V.; Sauve, G.; Guldi, D. M.; Asmus, K. D. *Res. Chem. Intermed.* **1997**, *23*, 575.

(55) Kamat, P. V.; Sauve, G.; Ruoff, R. S. *J. Phys. Chem.* **1995**, *99*, 2162.

(56) Mohan, H.; Palit, D. K.; Mittal, J. P.; Chiang, L. Y.; Asmus, K. D.; Guldi, D. M. *J. Chem. Soc., Faraday Trans.* **1998**, *94*, 359.

(57) Palit, D. K.; Mohan, H.; Birkett, P. R.; Mittal, J. P. *J. Phys. Chem. A* **1997**, *101*, 5418.

(58) Palit, D. K.; Mohan, H.; Mittal, J. P. *J. Phys. Chem. A* **1998**, *102*, 4456.

(59) Bensasson, R. V.; Hill, T. J.; Land, E. J.; Leach, S.; McGarvey, D. J.; Truscott, T. G.; Ebbenboch, J.; Gorst, M.; Rucharit, C. *Chem. Phys.* **1997**, *215*, 111.

(60) Sun, Y.-P.; Riggs, F. J.; Lin, B. *Chem. Mater.* **1997**, *9*, 1268.

(61) Signorini, R.; Zerbetto, M.; Meneghetti, M.; Bozio, R.; Maggini, M.; Faveri, C. D.; Prato, M.; Scorrano, G. *J. Chem. Soc., Chem. Commun.* **1996**, 1891.

(62) Birkett, P. R., unpublished results, manuscript in preparation.

(63) (a) Catalan, J.; Elguero, J. *J. Am. Chem. Soc.* **1993**, *115*, 9249. (b) Luo, C.; Fujitsuka, M.; Watanabe, A.; Ito, O.; Gan, L.; Huang, Y.; Huang, C.-H. *J. Chem. Soc., Faraday Trans.* **1998**, *94*, 527.

(64) Land, E. J.; Bensasson, R. V.; Truscott, T. G. In *Flash Photolysis and Pulse Radiolysis Contribution to the Chemistry, Biology and Medicine*; Pergamon Press: Oxford, 1983.

(65) Carmichael, I.; Hug, G. L. *J. Phys. Chem. Ref. Data* **1986**, *15*, 1.

(66) Murov, S.; Carmichael, I.; Hug, G. L. *Handbook of Photochemistry*; Marcel Dekker: New York, 1993.

(67) Amouyal, E.; Bensasson, R. V.; Land, E. J. *Photochem. Photobiol.* **1974**, *20*, 415.

(68) Dimitrijevic, N. M.; Kamat, P. V. *J. Phys. Chem.* **1992**, *96*, 4811.

(69) Palit, D. K.; Ghosh, H. N.; Pal, H.; Sapre, A. V.; Mittal, J. P.; Seshadri, R.; Rao, C. N. R. *Chem. Phys. Lett.* **1992**, *205*, 395.

(70) Senson, R. J.; Szarka, A. Z.; Smith, G. R.; Hochstrasser, R. M. *Chem. Phys. Lett.* **1991**, *185*, 179.

(71) Benesi, H. A.; Hildebrand, J. H. *J. Am. Chem. Soc.* **1949**, *71*, 2700.

(72) Ghosh, H. N.; Pal, H.; Sapre, A. V.; Mittal, J. P. *J. Am. Chem. Soc.* **1993**, *115*, 11722.

(73) Shida, T. *Electronic Absorption Spectra of the Radical Ions*; Elsevier, Amsterdam, 1985.

(74) Johnston, L. J.; Redmond, R. W. *J. Phys. Chem.* **1997**, *101*, 4660.

(75) Fujitsuka, M.; Luo, C.; Ito, O. *J. Phys. Chem. B* **1999**, *103*, 445.

(76) (a) Miyasaka, H.; Ojima, S.; Mataga, N. *J. Phys. Chem.* **1989**, *93*, 3380. Ojima, S.; Miyasaka, H.; Mataga, N. *J. Phys. Chem.* **1990**, *94*, 5834. Ashai, T.; Mataga, N. *J. Phys. Chem.* **1990**. (b) Ojima, S.; Miyasaka, H.; Mataga, N. *J. Phys. Chem.* **1990**, *94*, 4147. Ojima, S.; Miyasaka, H.; Mataga, N. *J. Phys. Chem.* **1990**, *94*, 7534.

(77) Nath, S.; Pal, H.; Palit, D. K.; Sapre, A. V.; Mittal, J. P. *J. Phys. Chem.* **1998**, *102*, 5418.